Clinical Infectious Diseases

BRIEF REPORT

Inherited Interleukin 2–Inducible T-Cell (ITK) Kinase Deficiency in Siblings With Epidermodysplasia Verruciformis and Hodgkin Lymphoma

Leila Youssefian,[1,2,3,a] Hassan Vahidnezhad,[1,4,a] Mehdi Yousefi,[5,6] Amir Hossein Saeidian,[1,3] Arghavan Azizpour,[7] Andrew Touati,[1,8] Neda Nikbakht,[1] Kambiz Kamyab-Hesari,[9] Mohammad Mahdi Adib-Sereshki,[10] Sirous Zeinali,[4,11] Behzad Mansoori,[12,13] Ali Jazayeri,[14] Razieh Karamzadeh,[15] Paolo Fortina,[16] Emmanuelle Jouanguy,[17,18,19] Jean-Laurent Casanova,[17,18,19,20,21] and Jouni Uitto[1]

[1]Department of Dermatology and Cutaneous Biology, Sidney Kimmel Medical College, and Jefferson Institute of Molecular Medicine, Thomas Jefferson University, Philadelphia, Pennsylvania; [2]Department of Medical Genetics, School of Medicine, Tehran University of Medical Sciences, Iran; [3]Genetics, Genomics and Cancer Biology PhD Program, Thomas Jefferson University, Philadelphia, Pennsylvania; [4]Biotechnology Research Center, Department of Molecular Medicine, Pasteur Institute of Iran, Tehran, [5]Department of Immunology, Faculty of Medicine and [6]Drug Applied Research Center, Tabriz University of Medical Sciences, and [7]Department of Dermatology, Razi Hospital, Tehran University of Medical Sciences, Iran; [8]Drexel University College of Medicine, Philadelphia, Pennsylvania; [9]Department of Pathology, Razi Hospital, Tehran University of Medical Sciences, [10]Gastrointestinal and Liver Diseases Research Center, Firoozgar Hospital, Iran University of Medical Sciences, and [11]Kawsar Human Genetics Research Center, Tehran, and [12]Immunology Research Center and [13]Student Research Committee, Tabriz University of Medical Sciences, Iran; [14]Department of Information Science, College of Computing and Informatics, Drexel University, Philadelphia, Pennsylvania; [15]Department of Stem Cells and Developmental Biology, Cell Science Research Center, Royan Institute for Stem Cell Biology and Technology, Academic Center for Education, Culture and Research, Tehran, Iran; [16]Cancer Genomics and Bioinformatics, Department of Cancer Biology, Sidney Kimmel Cancer Center, Thomas Jefferson University, Philadelphia, Pennsylvania; [17]St Giles Laboratory of Human Genetics of Infectious Diseases, Rockefeller Branch, Rockefeller University, New York, New York; [18]Laboratory of Human Genetics of Infectious Diseases, Necker Branch, Inserm U1163, Necker Hospital for Sick Children, and [19]Imagine Institute, Paris Descartes University, France; [20]Howard Hughes Medical Institute, New York, New York; and [21]Pediatric Hematology and Immunology Unit, Assistance Publique–Hôpitaux de Paris, Necker Hospital for Sick Children, Paris, France

Biallelic mutations in the *ITK* gene cause a T-cell primary immunodeficiency with Epstein-Barr virus (EBV)–lymphoproliferative disorders. We describe a novel association of a homozygous *ITK* mutation with β–human papillomavirus (HPV)–positive epidermodysplasia verruciformis. Thus, loss of function in ITK can result in broad dysregulation of T-cell responses to oncogenic viruses, including β-HPV and EBV.

Keywords. epidermodysplasia verruciformis; primary immunodeficiency; ITK; human papillomavirus; EBV infection.

Received 8 May 2018; editorial decision 25 October 2018; published online February 19, 2019.

[a]L. Y. and H. V. contributed equally to this work.

Correspondence: J. Uitto, Department of Dermatology and Cutaneous Biology, Sidney Kimmel Medical College at Thomas Jefferson University, 233 S 10th St, Suite 450 BLSB, Philadelphia, PA 19107 (jouni.uitto@jefferson.edu).

Clinical Infectious Diseases® 2019;XX(XX):1–4

DOI: 10.1093/cid/ciy942

Cutaneous human papillomavirus (HPV) infection typically manifests with isolated papillomas. However, some patients in familial clustering develop extensive and protracted HPV infections, primarily the β-HPV types 5 and 8, with distinct cutaneous findings [1–3]; β-HPVs do not cause lesions in the general population. This clinical entity, epidermodysplasia verruciformis (EV), with autosomal recessive inheritance, is characterized by numerous cutaneous flat warts in childhood, which progress into verrucous tumors and evolve into squamous cell carcinomas later in life. The "typical" form of EV, not vulnerable to other infections, is caused by mutations in *CIB1*, *TMC6*, or *TMC8*, which impair keratinocyte-intrinsic immunity to β-HPV infection [3–5]. Mutations in other genes have been associated with "atypical" EV (Supplementary Table 1) [1–3]. Defects in those genes impair T-cell development or function, predisposing to β-HPV and other infections [1, 2]. We now describe an extended family with atypical EV in association with a mutation in an additional T-cell gene, *ITK*, encoding interleukin 2–inducible T-cell kinase (ITK).

METHODS

Case Report

The proband, a 44-year-old Iranian woman born to first-cousin parents, presented with multiple flat warts scattered on her whole body, prominently on the hands and legs, noted since age 17 (Figure 1A and Supplementary Figure 1). Histopathology of a skin lesion was consistent with EV (Figure 1B), and was positive for HPV types 5 and 8 (Figure 1C). Viral typing also demonstrated the presence of Epstein-Barr virus (EBV) in plasma with a load of 10 000 IU/mL. The proband's younger sibling, a 40-year-old man (III-5 in Figure 1E), was diagnosed with Hodgkin lymphoma by computed tomographic scan showing a large peritoneal mass, and a needle biopsy confirmed the diagnosis (Supplementary Figure 1*D* and 1*E*). Clinical examination of skin, HPV typing, and histopathology of his skin lesions, similar to those in the proband, confirmed the diagnosis of EV. He also had high EBV load in plasma (Figure 1C). Both patients, therefore, suffered from atypical EV, associated with uncontrolled β-HPV and EBV infection. Short-term treatment with oral acitretin (10 mg/day) or local cryosurgery for skin lesions was largely ineffective. For Hodgkin disease, the patient received chemotherapy with ABVD (Adriamycin, Bleomycin, Vinblastine, Dacarbazine) protocol, which resulted in dramatic resolution of the intra-abdominal lymphadenopathies.

Whole Exome Sequencing

DNA was isolated from peripheral blood of the patients and family members, and DNA from 2 patients (III-3 and III-5)

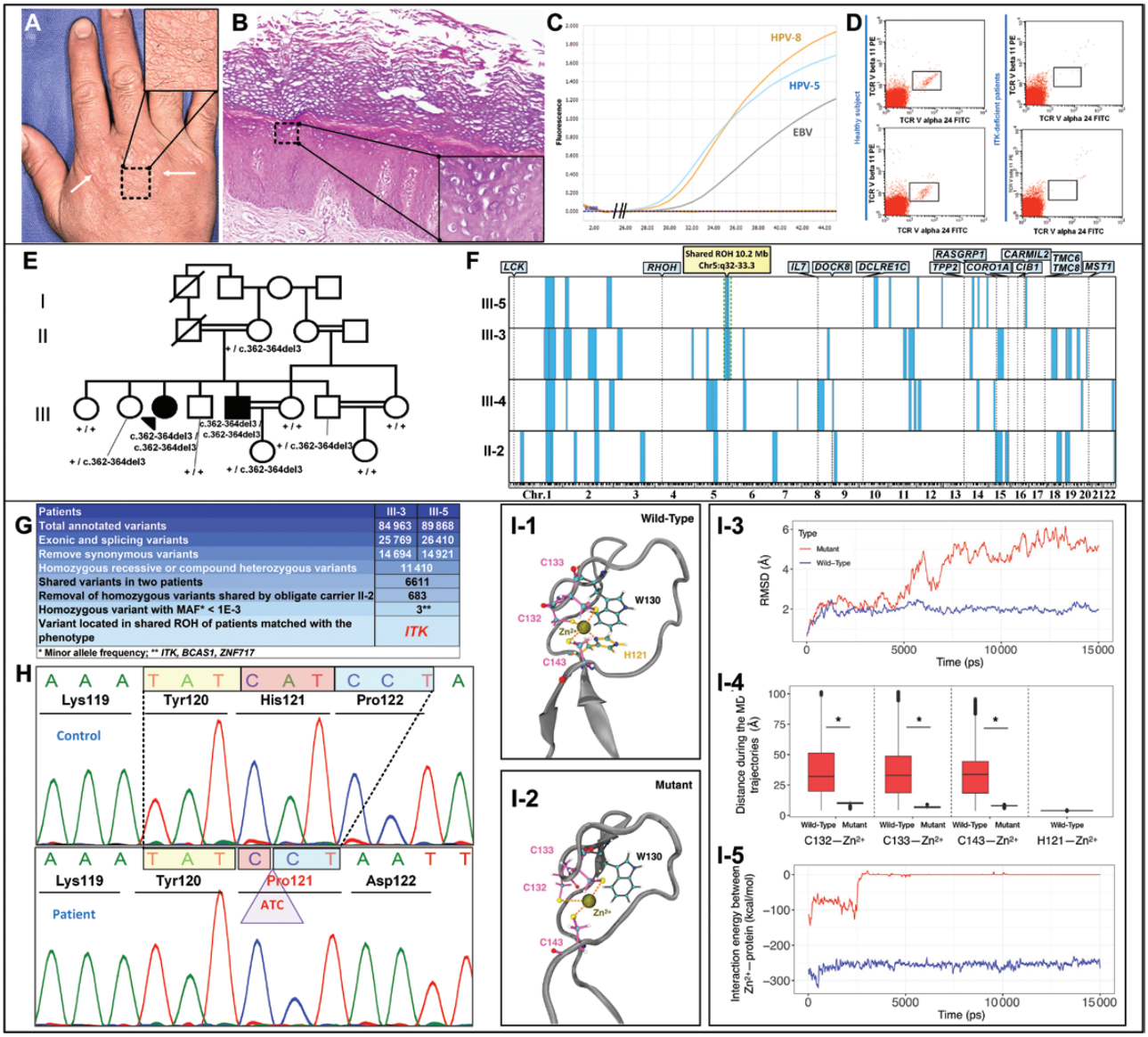

Figure 1. Strategy for identification of the homozygous *ITK* mutation in a family with epidermodysplasia verruciformis (EV). *A*, Clinical presentation of EV manifesting with flat warts (arrows) on the hands of patient III-5. *B*, Histopathology of a flat wart in acral skin from patient III-3. Note epidermal thickening with hyperkeratosis, acanthosis, and hypergranulosis (hematoxylin and eosin staining, ×10 magnification); note koilocytes with large cytoplasmic halo (inset, ×40). *C*, Viral typing by real time quantitative polymerase chain reaction from a skin biopsy revealed the presence of human papillomavirus types 5 and 8, while Epstein-Barr virus was present in plasma (viral load, 10 000 IU/mL) of both patients III-5 and III-3 (data from III-3 is shown). *D*, Fluorescence-activated cell sorting of $CD3^+$ T cells in patients III-3 and III-5 (upper and lower right panels, respectively) for T-cell receptor (TCR)–V$\alpha 24^+$ and TCR-V$\beta 11^+$. Reduced percentage of cells with these markers in patients with the *ITK* mutation (right panels: <0.02%), in comparison to 2 healthy controls (left panels: 0.36% and 0.42%), indicated lack of natural killer T cells. *E*, Pedigree of the family. Segregation analysis of the mutation is shown, with + sign representing the wild-type allele. *F*, Genome-wide homozygosity mapping was performed in patients III-3 and III-5, as well as in the healthy brother III-4 and the mother II-2. Regions of homozygosity (ROH) are represented by the blue vertical lines. The only ROH shared between the patients and not present in the unaffected individual was of 10.2 Mb on chromosome 5, containing the *ITK* locus. Locations of genes associated with EV are shown with black dotted lines. *G*, Whole exome sequencing and filtering of variants in patients III-3 and III-5, and the mother, II-2. Filtering criteria used to arrive at the pathogenic mutation in *ITK* are shown. *H*, Sanger sequencing confirmed that the c.362_364del mutation in *ITK* is homozygous in patient III-3 (lower panel); control DNA showed wild-type alleles only (upper panel). *I*, Structural analysis of the wild-type (*I*-1) and mutant (*I*-2) ITK protein motif in 3D structure. Interactions of Zn^{2+} ion with amino acids in the Cys_3His_1 motif are represented by orange dashed lines. Oxygen, hydrogen, nitrogen, sulphur, and carbon atoms are in red, white, blue, yellow, and cyan, respectively (stick-and-ball structures in *I*-1 and *I*-2). Backbone root-mean-square deviation (*I*-3), pairwise distance between Cys132–Zn^{2+}, Cys133–Zn^{2+}, Cys143–Zn^{2+}, and His121–Zn^{2+} (*I*-4). Wilcoxon signed-rank test significance: $*P < 2.2x10^{(-16)}$. Interaction energies of Zn^{2+} –Btk motif during the molecular dynamics trajectories in wild-type (blue line) and mutant (red line) structures (*I*-5). Abbreviations: EBV, Epstein-Barr virus; FITC, fluorescein isothiocyanate; HPV, human papillomavirus; ITK, interleukin 2–inducible T-cell kinase; MAF, minor allele frequency; MD, molecular dynamics; PE, phycoerythrin; RMSD, root-mean-square deviation; ROH, region of homozygosity; TCR, T-cell receptor.

and the patients' mother (II-2) was submitted to whole exome sequencing (WES). Exons and flanking intronic regions of approximately 20 000 genes (45 Mb; 98% of consensus coding sequence exons) were captured by the Illumina TruSeq

Exome Enrichment Kit and sequenced on a NextSeq 500 instrument (Illumina, San Diego, California). The data were analyzed as detailed in Figure 1G and the Supplementary Materials.

Homozygosity Mapping

Whole genome–wide single nucleotide polymorphism (SNP)–based homozygosity mapping was performed with DNA from 2 patients (III-3 and III-5) and their unaffected brother (III-4) and mother (II-2) by Infinium Global Screening Array-24 version 1.0 kit (~640 000 SNP markers; Illumina). The SNP genotyping data were analyzed by using PLINK (http://pngu.mgh.harvard.edu/) [6]. The regions of homozygosity (ROH) of ≥4 Mb were identified by an algorithm in PLINK.

Viral Typing

Skin and whole blood were collected from patients III-3 and III-5. Viral DNA was isolated with the High Pure viral nucleic acid extraction kit (Roche Diagnostic, Risch-Rotkreuz, Switzerland), followed by real time quantitative polymerase chain reaction by SYBR Green (Molecular Probes, Eugene, Oregon) for HPV types 5, 6, 8, 20, 21, and 38, as well as EBV, at 40 cycles of 30 seconds at 95°C, 60°C, and 72°C.

Fluorescence-activated Cell Sorting for Peripheral Blood Mononuclear Cell Immunophenotyping

Peripheral blood mononuclear cells (PBMCs) from whole blood from patients III-3 and III-5, as well as healthy controls, were isolated by density gradient centrifugation on Ficoll-Paque. CD3 MicroBeads were used to isolate T cells (Miltenyi Biotech, Bergisch-Gladbach, Germany). After gating on 1×10^5 $CD3^+$ T-cell lymphocytes, the percentage of natural killer (NK) T cells ($CD3^+$TCR-V$\alpha24^+$ TCR-V$\beta11^+$) was determined using the BD FACSCalibur (BD Biosciences, Singapore). Staining for fluorescence-activating cell sorting (FACS) was performed with fluorochrome-conjugated monoclonal antibodies (clones): CD3 (SK7; BD), TCR-Vα24 (C15), and TCR-Vβ11 (C21; Coulter-Immunotech, Miami, Florida).

T-Cell Proliferation Assay

Isolated PBMCs, 2×10^5 per well from the patients and unrelated healthy controls, were cultivated in Roswell Park Memorial Institute 1640 medium supplemented with 10% fetal bovine serum. Cultures were stimulated by 5 µg/mL phytohemagglutinin (PHA). After 72 hours of incubation, the treated and untreated cells were imaged under light microscope, and the cultures were examined by (3-(4,5-dimethylthiazol-2-yl)-2,5-diphenyltetrazolium bromide) assay during the last 24 hours of incubation.

Homology Modeling and Molecular Dynamics Simulations

Structural analysis of ITK in mutant and wild-type conformation was accomplished based on NMR structure of BTK motif (PDBID:2E6I). Mutant structure was modeled using the I-TASSER web server [7], and explicit molecular dynamics (MD) simulations were performed using the NAMD.2.12 package [8]. For details, see the Supplementary Materials.

RESULTS

Blood samples were collected from 11 family members, and DNA from patients III-3 and III-5 and their unaffected mother (II-2) was submitted for WES. WES data analysis, including multistep filtering of the variants, led to identification of homozygous variants in 3 candidate genes, *ITK*, *BCAS1*, and *ZNF717* (Figure 1G); of these genes, only *ITK* is known to be related to immunity [9, 10], and mutations in *ITK* have previously been associated with EBV infection and lymphoproliferative syndrome 1 (Online Mendelian Inheritance in Man number 613011) [11].

Homozygosity mapping was performed in patients (III-3 and III-5) as well as healthy relatives (III-4 and II-2) (Figure 1E). Only a single 10.2-Mb ROH was shared by both patients, but not present in healthy family members (Figure 1F). This ROH on chromosome 5 harbors the candidate gene *ITK*, and not *BCAS1* or *ZNF717*, providing additional evidence for causality of *ITK* mutations. The mutation in *ITK* (NM_005546) identified by WES and confirmed by Sanger sequencing, was a 3-bp deletion, c.362_364del (p.His121del) on exon 4 residing in a BTK-type zinc finger domain (aa119–148) containing the conserved histidine 121 (Figure 1H). This mutation was predicted to be disease causing in MutationTaster database, and it is not found either in ExAC, 1000 Genomes or gnom AD. Subsequent segregation analysis of 11 family members confirmed the homozygous *ITK* mutation as the associated variant (Figure 1E).

NK T cells are deficient in the peripheral blood of patients with *ITK* mutations [12, 13]. Immunophenotyping for NK T cells performed in our patients revealed a low number of NK T cells (Figure 1D). In contrast, FACS analysis revealed that the fraction of T cells expressing CD3 was normal (66.6 ± 1.08%) (Supplementary Figure 2). Finally, the T-cell proliferation assay showed that PHA-treated cells were capable of expanding and forming colonies, and there were no differences between the patients' and control cells. These observations are consistent with previous reports (Chung et al [13] and Çağdaş et al [14]) (Supplementary Figure 3).

To examine the consequences of His121 deletion on structural dynamics of the BTK motif, MD simulation was performed after induction of the mutation using homology modeling approach. Zn^{2+} ion forms coordination complexes with 4 residues (ie, Cys132, Cys133, Cys143, and His121) in a tetrahedral geometry in the wild-type structure (Figure 1I-1). Lack of His121 resulted in elimination of 1 of the 4 Zn^{2+} interactions (Figure 1I-2). To assess structural stability of wild-type and mutant conformations, both proteins were monitored during the 15 ns MD trajectories (Supplementary Table 2). Deletion of His121 led to instability of the BTK

motif as indicated by large fluctuations of backbone root-mean-square deviation in mutant conformation (Figure 1I-3). Since His121 is located at the conserved motif of zinc-finger domain (Cys_3His_1) assembly around a Zn^{2+} ion [15], we measured the distances between the center geometry of these residues and Zn^{2+} during the MD trajectories in both conformations. Figure 1I-4 indicates the pairwise distance between Cys132–Zn^{2+}, Cys133–Zn^{2+}, Cys143–Zn^{2+}, and His121–Zn^{2+}. Deletion of His121 in mutant ITK significantly increased the average distance between cysteine residues and Zn^{2+}. The interaction energies between the Zn^{2+} ion and protein at the initial stage of MD simulations were lower than in the wild-type form (–144 vs –321 kcal/mol, respectively) (Figure 1I-5), demonstrating the essential role of His121 in stability of the structure. By continuing the simulation, Zn^{2+} was released from the mutant protein, while it remained bound to wild-type (–0.2 ± 2.7 kcal/mol vs –254 ± 7.0 kcal/mol, respectively) (Supplementary Video).

DISCUSSION

Collectively, our data suggest that the homozygous *ITK* mutation is responsible for the EV and EBV phenotypes in this family. The *ITK* gene product ITK is a nonreceptor tyrosine kinase involved in T-cell receptor signaling [9, 10]. In mice, ITK plays a role in NK T and T-cell (αβ and γδ) development, activation, and function [9, 16]. Mutations in *ITK* have previously been reported in association with EBV lymphoproliferative disorders (LPDs) [12, 14, 17, 18]. Our demonstration of previously unpublished *ITK* mutations in EV is novel, as susceptibility to β-HPV infection has not been reported in association with this gene. Additionally, the presence of EV in patient III-3, who did not have EBV-LPD, suggests that predisposition to cutaneous HPV infection is primarily related to loss of ITK, and not secondary to immune dysfunction from EBV-LPDs. Finally, association between β-HPV and EBV diseases has been reported in patients with other T-cell aberrations [19]. Consequently, it would be prudent to genotype all EV patients with documented β-HPV infection for mutations, potentially prognosticating the development of LPDs and assisting in planning for appropriate anticancer treatments.

Supplementary Data

Supplementary materials are available at *Clinical Infectious Diseases* online. Consisting of data provided by the authors to benefit the reader, the posted materials are not copyedited and are the sole responsibility of the authors, so questions or comments should be addressed to the corresponding author.

Notes

Acknowledgments. The authors thank the family for cooperation. Carol Kelly assisted in manuscript preparation.

Financial support. This study was supported by the institutional funds of the Department of Dermatology and Cutaneous Biology of Thomas Jefferson University. The laboratory of Human Genetics of Infectious Diseases was supported by the National Institute of Health (R21 AI107508-02), The Rockefeller University, Institut National de la Santé et de la Recherche Médicale, Paris Descartes University, and the St. Giles Foundation.

Potential conflicts of interest. J.-L. C. has received personal fees from Genentech, ADMA Biologics, Nimbus, Vitae Pharmaceuticals, Kymera Therapeutics, Sanofi, Asahi Kasei, and Pfizer. All other authors report no potential conflicts. All authors have submitted the ICMJE Form for Disclosure of Potential Conflicts of Interest. Conflicts that the editors consider relevant to the content of the manuscript have been disclosed.

References

1. Uitto J, Vahidnezhad H. Expanding genetics and phenotypic spectrum of epidermodysplasia verruciformis. Br J Dermatol **2016**; 175:1138–9.
2. Przybyszewska J, Zlotogorski A, Ramot Y. Re-evaluation of epidermodysplasia verruciformis: reconciling more than 90 years of debate. J Am Acad Dermatol **2017**; 76:1161–75.
3. de Jong SJ, Imahorn E, Itin P, et al. Epidermodysplasia verruciformis: inborn errors of immunity to human beta-papillomaviruses. Front Microbiol **2018**; 9:Article 1222:1–9.
4. de Jong SJ, Créquer A, Matos I, et al. The human CIB1-EVER1-EVER2 complex governs keratinocyte-intrinsic immunity to β-papillomaviruses. J Exp Med **2018**; 215:2289–310.
5. Youssefian L, Vahidnezhad H, Mahmoudi H, et al. Epidermodysplasia verruciformis: genetic heterogeneity and EVER1 and EVER2 mutations revealed by genome-wide analysis. J Invest Dermatol **2018**. doi:10.1016/j.jid2018.07.010.
6. Vahidnezhad H, Youssefian L, Jazayeri A, Uitto J. Research techniques made simple: genome-wide homozygosity/autozygosity mapping is a powerful tool for identifying candidate genes in autosomal recessive genetic diseases. J Invest Dermatol **2018**; 138:1893–900.
7. Yang J, Yan R, Roy A, Xu D, Poisson J, Zhang Y. The I-TASSER suite: protein structure and function prediction. Nat Methods **2014**; 12:7–8.
8. Phillips JC, Braun R, Wang W, et al. Scalable molecular dynamics with NAMD. J Comput Chem **2005**; 26:1781–802.
9. August A, Ragin MJ. Regulation of T-cell responses and disease by tec kinase Itk. Int Rev Immunol **2012**; 31:155–65.
10. Ghosh S, Drexler I, Bhatia S, Gennery AR, Borkhardt A. Interleukin-2-inducible T-cell kinase deficiency-new patients, new insight? Front Immunol **2018**; 9:979.
11. Bienemann K, Borkhardt A, Klapper W, Oschlies I. High incidence of Epstein-Barr virus (EBV)–positive Hodgkin lymphoma and Hodgkin lymphoma-like B-cell lymphoproliferations with EBV latency profile 2 in children with interleukin-2-inducible T-cell kinase deficiency. Histopathology **2015**; 67:607–16.
12. Huck K, Feyen O, Niehues T, et al. Girls homozygous for an IL-2-inducible T cell kinase mutation that leads to protein deficiency develop fatal EBV-associated lymphoproliferation. J Clin Invest **2009**; 119:1350–8.
13. Chung BK, Tsai K, Allan LL, et al. Innate immune control of EBV-infected B cells by invariant natural killer T cells. Blood **2013**; 122:2600–8.
14. Çağdaş D, Erman B, Hanoğlu D, et al. Course of IL-2-inducible T-cell kinase deficiency in a family: lymphomatoid granulomatosis, lymphoma and allogeneic bone marrow transplantation in one sibling; and death in the other. Bone Marrow Transplant **2017**; 52:126–9.
15. Krishna SS, Majumdar I, Grishin NV. Structural classification of zinc fingers: survey and summary. Nucleic Acids Res **2003**; 31:532–50.
16. Prince AL, Yin CC, Enos ME, Felices M, Berg LJ. The Tec kinases Itk and Rlk regulate conventional versus innate T-cell development. Immunol Rev **2009**; 228:115–31.
17. Ghosh S, Bienemann K, Boztug K, Borkhardt A. Interleukin-2-inducible T-cell kinase (ITK) deficiency—clinical and molecular aspects. J Clin Immunol **2014**; 34:892–9.
18. Cipe FE, Aydogmus C, Serwas NK, et al. ITK deficiency: how can EBV be treated before lymphoma? Pediatr Blood Cancer **2015**; 62:2247–8.
19. Platt CD, Fried AJ, Hoyos-Bachiloglu R, et al. Combined immunodeficiency with EBV positive B cell lymphoma and epidermodysplasia verruciformis due to a novel homozygous mutation in RASGRP1. Clin Immunol **2017**; 183:142–4.